ASEAN Journal of Chemical Engineering 2026, Vol. 26, No. 1, 145 – 165

Cassava Starch-Based Biocomposites Reinforced with Zinc Oxide and Spent Coffee Ground Cellulose: A Comparative Study and TOPSIS Evaluation

Nyoman Puspa Asri *
Hans Rachman
Jaclyn Regina Anggara
Raymond Hamidy
Jessica Renata Yoewono
Yohannes Somawiharja
Food Technology Program, Faculty of Tourism, Ciputra University Surabaya, Surabaya, Indonesia
*e-mail: nyoman.asri@ciputra.ac.id

Submitted 5 August 2025 *Revised* 13 April 2026 *Accepted* 15 April 2026

Abstract. The accumulation of synthetic plastic waste and depletion of fossil resources have driven the search for sustainable alternatives, such as biodegradable bioplastics. This study explores the use of cellulose derived from spent coffee grounds (SCG) and zinc oxide (ZnO) as reinforcing fillers in cassava starch-based bioplastics fabricated via solution-casting methods. Various formulations were developed using SCG cellulose (1%, 1.5%, and 2% with 10%, 15%, and 20% glycerol) or ZnO (1%, 1.5%, and 2% with 10% and 15% glycerol) The resulting films were evaluated for their mechanical, barrier, and optical properties, followed by structural analysis using Fourier Transform Infrared Spectroscopy (FTIR), X-ray Diffraction (XRD), and Scanning Electron Microscopy (SEM). Results showed that SCG-based cellulose significantly improved tensile strength (up to 1.87 MPa) but reduced transparency (to 46.38%), while ZnO-enhanced films exhibited higher light transmittance (up to 70.28%). FTIR confirmed hydrogen bonding interactions between the filler and the starch matrix, and XRD revealed differences in crystallinity, with cellulose showing semi-amorphous characteristics and ZnO contributing to higher peak intensity. SEM analysis supported these findings, indicating a more compact and continuous matrix in ZnO films. A multi-criteria decision-making analysis using the TOPSIS method identified the optimal cellulose-based formulation as 2% SCG cellulose with 20% glycerol, which achieved a tensile strength of 1.87 MPa, transparency of 46.40, and a water vapor permeability (WVP) of 2.318 × 10-6 g/m·day·Pa. These findings demonstrate the potential of SCG and ZnO as functional additives in biodegradable packaging materials and support the circular economy by valorizing organic waste.

Keywords: Bioplastic, Cellulose, Spent Coffee Ground, TOPSIS, Zinc oxide

INTRODUCTION

Plastics are integral to modern life and are widely used across various industrial sectors due to their practicality, low cost, ease of processing, and corrosion resistance (Folino *et al.*, 2023). However, most conventional plastics are derived from non-renewable petroleum-based resources, contributing significantly to fossil fuel depletion and

DOI: 10.22146/ajche.23638

environmental pollution. In addition to being non-biodegradable, the plastic lifecycle—spanning production to disposal—accounts for approximately 4.5% of global greenhouse gas emissions (Cabernard *et al.,* 2022).

In 2022, global plastic production reached 400.3 million tons and is projected to rise exponentially in the coming years (Nayanathara Thathsarani Pilapitiya and Ratnayake, 2024). Without adequate waste management systems, the accumulation of plastic waste threatens both terrestrial and marine ecosystems (Ali *et al.,* 2023). This growing crisis underscores the urgent need to develop environmentally friendly alternatives, such as bioplastics. Various bio-based materials, including polysaccharides, polyhydroxyalkanoates (PHA), polylactic acid (PLA), seaweed, and mycelium, have been explored for bioplastic production (Atiwesh *et al.,* 2021). Among these, cellulose is especially attractive due to its abundance, biodegradability, and high mechanical strength. As a reinforcing filler, cellulose possesses a high crystallinity index and a surface rich in hydroxyl (-OH) groups. These functional groups allow the formation of a robust hydrogen-bonded network with the starch chains, thereby enhancing the load-bearing capacity and thermal stability of the resulting biocomposite (Abe *et al.,* 2021; Khouaja *et al.,* 2025). It is widely distributed in plant biomass, with content ranging from 1% to 95% depending on the source (Hernandez & Rosa, 2016).

Spent coffee grounds (SCG), a by-product of the coffee industry, offer a promising source of cellulose for bioplastic production. As one of the most consumed beverages globally, coffee generates significant amounts of waste, with annual production estimated at around 168 million tons (Viana Freitas *et al.,* 2024). Approximately 650 kg of SCG are produced per ton of coffee beans processed (Karmee, 2018). Containing up to 12.4% cellulose, SCG is a viable and cost-effective resource for biopolymer extraction (Singh *et al.,* 2023) and contributes to waste reduction and circular economy initiatives.

Zinc oxide (ZnO) is another promising additive frequently incorporated into bioplastics. ZnO is known to enhance the mechanical and barrier properties of biopolymer matrices (Abdullah et al., 2020). Additionally, it exhibits antimicrobial activity by generating reactive oxygen species (ROS) that induce oxidative stress in microbial cells (Klink *et al.,* 2022). Its capacity to absorb ultraviolet (UV) radiation also makes ZnO a suitable additive for bioplastics intended for food packaging, as it helps protect contents from photodegradation (Liu *et al.*, 2024).

Previous research has explored the integration of ZnO with various bioplastic matrices, such as canna tuber starch (Hasna *et al.,* 2022), sugarcane-derived carboxymethyl cellulose (Vyas *et al.,* 2025), banana starch (Sapei *et al.,* 2017), and pineapple leaf fiber (Armynah *et al.,* 2022). Likewise, cellulose is extracted from diverse sources, including banana stems (Devika & Saha, 2024), algae (Steven *et al.,* 2022), pine wood (Dibha *et al.,* 2023), and bacterial fermentation (Gea *et al.,* 2022). It has been widely investigated. However, limited studies have systematically evaluated the individual performance of SCG-derived cellulose and ZnO as separate reinforcing fillers in a starch-based system. This study seeks to bridge this gap by investigating the properties of bioplastics reinforced with either SCG-based cellulose or ZnO. Specifically, the formulations varied the concentration of SCG cellulose (1%, 1.5%, and 2% with 10–20% glycerol) and ZnO (1%, 1.5%, and 2% with 10–15% glycerol). The optimal formulation for

each filler type was then determined using the TOPSIS method to achieve desirable mechanical strength, transparency, and water vapor permeability. This work contributes to the development of sustainable packaging materials while promoting the valorization of agro-industrial waste.

MATERIALS AND METHODS

Materials

The materials used in this research included arabica SCG (Indonesia) from local cafe, cassava strach (food grade, Rose Brand, Indonesia), glycerol (analytical grade, Indonesia), ZnO (Merck, Germany), KOH (Merck, Germany), H_2O_2 50% (Solvay, Belgium), CH_3COOH (Merck, Germany), NaOH (Merck, Germany), CH_4N_2O (ROFA, Indonesia).

Instruments

The equipment used in this research included a hotplate (VELP Scientifica, Italy), oven (Memmert, Germany), centrifuge NF-800R (Nüve, Turkey), scanning electron microscope FlexSEM 1000 (Hitachi, Japan), fourier transform infrared spectroscopy IRTracer 1000 (Shimadzu, Japan), x-ray diffraction Miniflex 600 (Rigaku, Japan), moisture analyzer (OHAUS, China), UV-Vis spectrophotometer SP-UV1100 (Dlab, USA), analytical balance ATX 224 (Shimadzu, Japan), and relative humidity (RH) meter (Elitech, China).

Cellulose Extraction from SCG

Extraction of Cellulose was carried out according to the method of Hamidy *et al.* (2025). Arabica SCGs were oven-dried at 105°C for 30 minutes, cooled in a desiccator, ground, and weighed. Afterward, dried SCGs were delignified using 3% KOH solution at 90°C for 2 hours under constant stirring. The resulting solids were washed and neutralized to a pH of 7. The sample is then bleached with a 10% H_2O_2 and 0.1 M NaOH solution for 45 minutes to remove color.

Bleached samples were neutralized and extracted using a 100 mL solution containing 8.5 g NaOH, 5 mL CH_3COOH, 8.5 g CH_4N_2O, and 100 mL distilled water at 70°C for 180 minutes under continuous stirring. The resulting cellulose was filtered, washed, and dried at 50°C for 24 hours to remove excess moisture. The extracted SCG-derived cellulose was ground and sieved to a uniform particle size (80-mesh, approx. 177 µm) before incorporation into the starch matrix.

Fabrication of Cellulose & ZnO Enriched Bioplastics

Bioplastic films were fabricated via solution casting (Vyas *et al.,* 2025).. For each formulation, 5 g of cassava starch was dispersed in 100 mL of distilled water. SCG-derived cellulose or ZnO was added as a reinforcing filler at concentrations of 1%, 1.5%, and 2% (w/w based on starch weight). Glycerol was incorporated as a plasticizer at 10%, 15%, and 20% (w/w) for cellulose-based films. In the case of ZnO-reinforced films, only 10% and 15% glycerol concentrations were utilized**,** as formulations with 20% glycerol resulted in highly brittle films that were unsuitable for characterization. The mixture was heated at 100°C with constant stirring (1500 rpm) for approximately 10 minutes until full gelatinization was achieved. The solution was then cast into 20 cm x 20 cm molds and dried at 50°C for 24 hours.

The resulting mixture was then evenly poured into a plastic casting measuring 27 × 19 cm. The tray is dehydrated in an oven at 60°C for 24 hours before further testing. The formulation of cellulose, ZnO, and Glycerol

used was based on Table 1. The 20% glycerol formulation for ZnO bioplastics is omitted due to the poor bioplastic result.

Table 1. Formulation of bioplastic

Glycerol (%)	Cellulose (%)	ZnO (%)
10	1	-
10	1.5	-
10	2	-
10	-	1
10	-	1.5
10	-	2
15	1	-
15	1.5	-
15	2	-
15	-	1
15	-	1.5
15	-	2
20	1	-
20	1.5	-
20	2	-

Physical Characterization

The thickness of the biofilm was determined according to the ASTM D6988 standard using screw micrometers with an accuracy of 0.01 mm (Vyas *et al.*, 2025). The biofilm density was then calculated based on Equation (1).

$$\rho = \frac{m}{A \times L} \quad (1)$$

where "ρ" is the bioplastic's density (in g/cm^3), "A" is the bioplastic's surface area (in cm^2), "L" is the bioplastic's thickness (in cm), and "m" is the mass of bioplastic (in g).

The moisture content of the bioplastic was determined using the thermogravimetric method with a moisture analyzer (Janas & Kowalska, 2023. One gram of the bioplastic sample was placed into the instrument and dried at 105°C. The moisture content is expressed in % wet basis (wb).

Mechanical Characterization

The tensile strength of bioplastic was determined using a texture analyzer according to Azlim *et al.* (2022). Bioplastic samples with dimensions of 2 × 8 cm were subjected to tensile testing at a pulling speed of 30 cm/min at a temperature of 25°C. The tensile strength of bioplastics was calculated as the maximum force (N) divided by the sample's cross-sectional area (width × thickness) and expressed in megapascals (MPa).

Optical Characterization

Absorbance of the bioplastic sheets was measured using a UV-vis spectrophotometer at 600 nm against a blank flask according to Benitez et al. (2024). The transparency of the bioplastic was determined from transmittance at that wavelength (T_{600}) using Beer-Lambert's law (Equation 2).

$$T_{600} = 10^{2-A} \quad (2)$$

where "T_{600}" is the bioplastic's transmittance (in %) and "A" is the bioplastic's absorbance at 600 nm (in cm).

Water Vapor Permeability

Water vapor permeability (WVP) of the bioplastic was determined according to ASTM E-96-00 using the gravimetric method, following the method of Mohammad Azmin *et al.* (2020) with modifications. Bioplastic sheets were placed to cover Erlenmeyer flasks containing 2 g of silica gel. The flasks were conditioned inside a desiccator (25°C, 75% relative humidity) using a saturated NaCl solution. WVP was determined as the weight gain of the desiccant after 48 h, according to Equation (3).

$$WVP = \frac{Q}{t} \times \frac{1}{A} \times \frac{L}{P_S(RH_1 - RH_2)} \quad (3)$$

where "WVP" is the bioplastic's water vapor permeability (in g m^{-1} day^{-1} Pa^{-1}), Q/t is the mass gain (g day^{-1}), "A" is the bioplastic's surface area (in m^2), "L" is the bioplastic's thickness (in m), P_s is the saturation pressure at 25°C (3.17 kPa), RH_1 is the relative humidity in the desiccator (75%), and RH_2 is the relative humidity inside the Erlenmeyer flask (in %).

Optimum Formulation Determination

The optimal formulation for both cellulose and ZnO-enriched bioplastics was determined using the TOPSIS (Technique for Order Preference by Similarity to Ideal Solution) method, as described by Ali *et al.* (2024). A decision matrix $(r_{ij})_{m\times n}$ was constructed where $i = 1,2,\dots,m$ represents the alternatives (bioplastic formulations), and $j = 1,2,\dots,n$ represents the evaluation criteria, which include tensile strength, transparency, and water vapor permeability (WVP). The matrix was normalized using vector normalization to eliminate differences in measurement scales, and weighted to obtain the weighted normalized matrix (v_{ij}) written in equation (4) where w_j denotes the weight of the criterion j.

$$v_{ij} = w_j r_{ij} \quad (4)$$

The positive ideal solution (IS) and negative ideal solution (NIS) were then determined based on the nature of each criterion. For benefit criteria (tensile strength and transparency), the ideal solution corresponds to the maximum value, whereas for the cost criterion (WVP), the ideal solution corresponds to the minimum value. Conversely, the negative ideal solution was defined using the opposite conditions. The separation distances between each alternative and both the ideal and negative-ideal solutions were calculated using the Euclidean distance, as expressed in Equations (5) and (6).

$$S_i^* = \sqrt{\sum_{j=1}^{n} (v_j^* - v_{ij})^2} \quad (5)$$

$$S_i^{**} = \sqrt{\sum_{j=1}^{n} (v_j^{**} - v_{ij})^2} \quad (6)$$

The relative closeness of each alternative to the ideal solution was then calculated as C_i, as shown in Equation (7), where values range from 0 to 1, with higher values indicating better performance. The formulation with the highest C_i value was selected as the optimal formulation.

$$C_i = \frac{S_i^{**}}{S_i^{**} + S_i^*} \quad (6)$$

The weights assigned to each criterion are shown in Table 2.

Table 2. TOPSIS weighing of bioplastic

Parameter	Weight (%)	Criteria
Tensile strength	40	Benefit
Transparency	30	Benefit
WVP	30	Cost

Subsequently, the optimum formulation for cellulose-ZnO bioplastics was further compared using a t-test and analyzed morphologically, chemically, and structurally.

Morphological Characterization

The surface morphology of the bioplastics was examined using a Scanning Electron Microscope (SEM) at an accelerating voltage of 3 kV. Prior to imaging, the samples were sputter-coated with a thin layer of gold to enhance conductivity. Observations were conducted at magnifications of 500× and 1000×.

Table 3. Physical properties of bioplastic

Parameter	Cellulose Concentration			ZnO Concentration		
	1%	1.5%	2%	1%	1.5%	2%
Thickness (mm)						
10% Glycerol	0.09±0.01^{c}	0.16±0.02^{ab}	0.12±0.02^{bc}	0.08±0.01^{ab}	0.09±0.01^{ab}	0.10±0.00^{a}
15% Glycerol	0.13±0.01^{abc}	0.14±0.01^{ab}	0.16±0.02^{a}	0.07±0.02^{b}	0.09±0.01^{ab}	0.09±0.01^{b}
20% Glycerol	0.15±0.01^{ab}	0.14±0.01^{ab}	0.15±0.00^{ab}	-	-	-
Density (g/cm^3)						
10% Glycerol	1.26±0.04^{a}	1.09±0.04^{cd}	1.05±0.02^{de}	1.79±0.11^{a}	1.52±0.06^{c}	1.60±0.06^{abc}
15% Glycerol	1.11±0.04^{cd}	0.81±0.01^{f}	0.97±0.04^{e}	1.54±0.12^{c}	1.76±0.03^{ab}	1.56±0.06^{bc}
20% Glycerol	1.17±0.03^{bc}	1.23±0.03^{ab}	0.86±0.01^{f}	-	-	-
Moisture Content (%)						
10% Glycerol	9.66±0.44^{ab}	9.06±0.70^{bc}	8.47±0.46^{c}	9.00±0.46^{a}	8.86±0.21^{a}	9.53±0.59^{a}
15% Glycerol	9.97±0.14^{ab}	9.02±0.49^{bc}	10.11±0.21^{ab}	9.14±0.22^{a}	8.96±0.62^{a}	9.92±0.76^{a}
20% Glycerol	10.45±0.32^{a}	9.07±0.28^{bc}	10.17±0.38^{ab}	-	-	-

Results are means of triplicate determinations ± standard deviation. The values in rows and columns with different letters are significantly different from each other ($P<0.05$)

Chemical Characterization

The infrared spectra of the bioplastic films were acquired using a Fourier-transform infrared (FTIR) spectrometer equipped with an attenuated total reflection (ATR) accessory. Spectra were recorded over 4000–500 cm^{-1} with a resolution of 4 cm^{-1} and averaged over 25 scans to improve signal-to-noise ratio.

The structural properties of the films were analyzed by X-ray diffraction (XRD), performed at an operating voltage of 40 kV and current of 150 mA. Measurements were conducted using a continuous 2θ scan over 5–70°.

Table 3 shows the physical characteristics of cellulose-based bioplastics. The cellulose-based bioplastics had thicknesses of 0.09-0.16 mm, densities of 0.81-1.26 g/cm^3, and moisture contents of 8.47%-10.45%. Cellulose is known to enhance the distribution of microcrystalline and promote interaction between the matrix and filler, thereby increasing compactness and, consequently, thickness (Nasution *et al.,* 2023; Oluwasina *et al.,* 2024). However, the results of this study indicate that density is not solely determined by cellulose concentration, as fluctuations were observed across different glycerol levels. In particular, a decrease in density at 20% glycerol suggests a dominant plasticizing effect. At higher concentrations, glycerol disrupts the intermolecular bonds, increasing free volume and decreasing its density (Fransiska *et al.,* 2024). Furthermore, the interaction between cellulose and glycerol, and the relatively large particle size of cellulose (80 mesh, approx. 177 µm), reduces packing efficiency within the matrix (Hamidy *et al.,* 2025). Because larger particles are harder to distribute uniformly, the voids tend to decrease the film's density.

Interestingly, at 20% glycerol and 1.5% cellulose, a relatively higher density was observed compared to other formulations at the same glycerol level. This may be attributed to a more optimal balance between filler concentration and plasticizer effect; as such, the cellulose is sufficiently dispersed without excessive aggregation (Safitri *et al.,* 2022). Therefore, the variations highlight the effects of particle size, filler

dispersion, and plasticizer on the film's structure

For ZnO-based bioplastics, thickness ranged from 0.07 to 0.10 mm, density from 1.52 to 1.79 g/cm^3, and moisture content from 8.86% to 9.92%. The addition of ZnO significantly affected thickness and density, while moisture content differences were less pronounced. The observed fluctuations in ZnO-based bioplastics follow a similar trend to those observed in cellulose-based systems, where non-linear behavior arises from competing effects within the matrix. However, in the case of ZnO, these variations are primarily associated with the dispersion–agglomeration behavior of inorganic particles and their interaction with the plasticized polymer network. Higher ZnO concentrations led to thicker and denser films, likely due to filler-matrix interactions (Abdullah *et al.,* 2020; Werapun *et al.*, 2024). Conversely, glycerol had a plasticizing and moisture-retaining effect, increasing thickness and moisture content but reducing density due to disruption of cellulose crystallinity (Nurhayati *et al.,* 2025)

Previous studies reported lower results, with a starch-based bioplastic containing ZnO having a density of 1.12-1.46g/cm^3 and a moisture content of 10.35-23.12% (Vyas *et al.,* 2025). The difference might be due to the use of ZnO nanoparticles. Another study on cellulose bioplastic showed that increasing the plasticizer content led to higher thickness (0.181–0.259 mm) and lower density (1.33–1.54 g/cm^3) (Nigam *et al.,* 2021). Moreover, the observed variations are also attributed to differences in mold surface area, particle size, and the agglomeration effect at higher filler concentrations (Putranti & Nugraheni, 2023).

Tensile Strength

Because it is made from biodegradable materials, bioplastic often has lower tensile strength than traditional plastic (Safitri *et al.,* 2022). Therefore, the formulated bioplastic needs to have adequate tensile strength. Figures 1 and 2 show that the tensile strength of bioplastics was significantly affected by the concentration of both cellulose and ZnO ($P < 0.05$). In the cellulose group, the highest tensile strength (1.87 ± 0.03 MPa) was observed in the 2% cellulose and 20% glycerol formulation, while the lowest (0.77 ± 0.20 MPa) was observed in the 1% cellulose and 10% glycerol formulation.

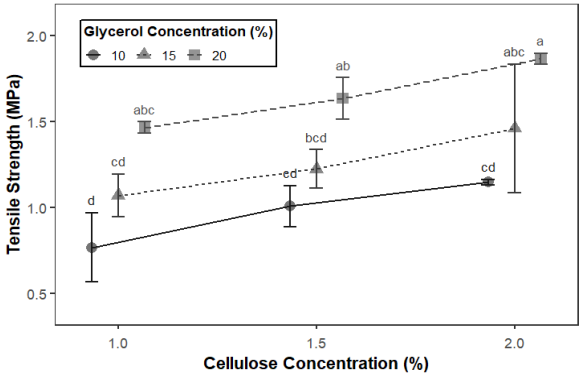


Fig. 1: Effect of cellulose & glycerol concentration on bioplastic tensile strength

Increasing cellulose content improved tensile strength due to its high crystallinity, which reinforces the starch matrix through effective stress transfer (Khouaja *et al.,* 2025). The abundant hydroxyl groups in cellulose can form strong intermolecular hydrogen bonds with starch chains, enhancing the mechanical integrity of the film (Popescu *et al.*, 2020; Abe *et al.,* 2021; Xie *et al.,* 2023). Additionally, glycerol may contribute to the formation of stable interactions among starch, glycerol, and cellulose, improving structural cohesion and minimizing brittleness (Gonçalves et al., 2019).

Similarly, the ZnO-based bioplastics showed tensile strengths ranging from 0.79 to 1.68 MPa, increasing with increasing ZnO

and glycerol concentrations. This improvement can be attributed to effective filler–matrix interactions and stress transfer when ZnO particles are well-dispersed within the matrix. However, the reinforcing effect is still governed by dispersion quality. At lower ZnO concentrations, the improvement in tensile strength is limited by insufficient filler content, whereas at higher concentrations, the risk of particle agglomeration remains. ZnO particles possess high surface energy, which can promote aggregation and create localized stress concentration points that weaken the material (Arifin *et al.,* 2022; Dadashi *et al.,* 2025).

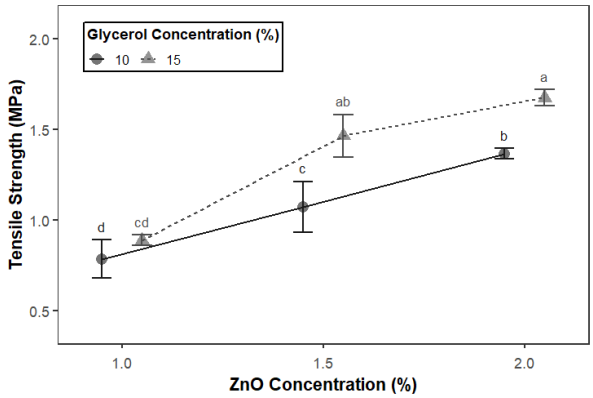


Fig. 2: Effect of ZnO & glycerol concentration on bioplastic tensile strength

Compared to previous studies, bioplastics produced in this research fall into the observed range commonly reported. Cellulose-reinforced bioplastics have been reported to exhibit tensile strengths ranging from 0.85 to 24.54 MPa through crosslinking and the use of nanoparticles (Rahmatullah *et al.,* 2022; Xie *et al.,* 2023). On the other hand, a study utilizing 4% ZnO achieved a tensile strength of 10.29 MPa (Abdullah *et al.,* 2020).

The comparatively lower tensile strength observed in this study may be attributed to several factors. First, the use of relatively large cellulose particle sizes (80 mesh, approx. 177 µm) likely limited effective stress transfer due to poor interfacial interaction and reduced dispersion compared to nanoscale reinforcements. Second, the absence of chemical crosslinking or surface modification may have resulted in weaker intermolecular bonding within the polymer matrix. In addition, the ZnO concentrations used in this study (≤2%) were lower than those reported in studies achieving higher mechanical strength, which may limit the reinforcing effect.

Transparency

Because it is frequently used for packaging other products, bioplastic needs to be transparent (Baltscheit *et al.,* 2020). To be classified as transparent, an object needs to have at least 80% transmittance, while a transmittance value between 10 and 80 % is considered opaque (Guzman-Puyol *et al.,* 2022). In this study, all treatments resulted in opaque bioplastic, indicated by the transmittance value at 600 nm. The transmittance of bioplastic films was significantly affected by the concentration of cellulose, ZnO, and glycerol ($P < 0.05$). In the cellulose group, the highest transmittance (69.18 ± 0.28%) was observed in the sample containing 1% cellulose and 10% glycerol (See Figure 3), while increasing cellulose concentration led to a gradual decrease in transparency. This reduction is attributed to the high refractive index and crystalline structure of cellulose, which scatters light and increases film opacity (Lounis *et al.,* 2024).

Similarly, bioplastics containing ZnO showed declining transparency with increasing ZnO and glycerol concentrations. The highest transmittance (70.28 ± 2.19%) was observed in the sample containing 1% ZnO and 15% glycerol, whereas the lowest (46.38 ± 0.77%) was observed in the sample containing 2% ZnO and 10% glycerol (See

figure 4). ZnO's high refractive index and nano-sized particles promote wide dispersion and light scattering, contributing to a cloudy appearance (Tamimi *et al.,* 2021). Additionally, excessive glycerol may saturate the starch matrix, leading to molecular phase separation and a hazy film structure, further reducing transparency (Sanyang *et al.,* 2016).

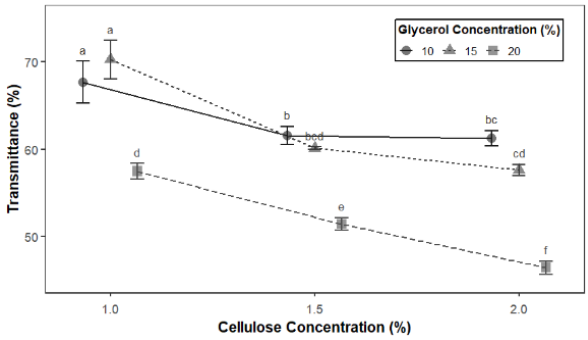


Fig. 3: Effect of cellulose & glycerol concentration on bioplastic transmittance

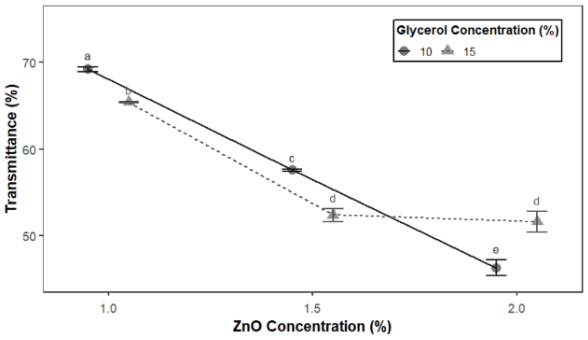


Fig. 4: Effect of ZnO & glycerol concentration on bioplastic transmittance

A previous study by Benitez *et al.* (2024) showed no significant difference in cellulose-glycerol bioplastic with different formulations with high transmittance (>90%). However, lower transmittance (35.48–38.3%) is reported by Krishnamurthy and Amritkumar (2019) for a starch-based bioplastic with different cross-linking compounds. Another study also showed that adding 0.6% cardanol reduced the transmittance of waxy corn starch bioplastic from 53.6% to 38.6% (Yahia *et al.,* 2024). This shows that bioplastic transparency is influenced by factors such as polymer type, additive presence, and the material's overall structure and crystallinity.

Water Vapor Permeability

Water vapor permeability (WVP) is the rate at which water vapor passes through a material under specific temperature and humidity conditions, typically driven by a vapor pressure gradient across a flat surface (Long *et al.,* 2023). Lower WVP values indicate greater resistance to moisture diffusion, which is essential for prolonging shelf life. This parameter is influenced by various factors, including film thickness, component polarity, density, structural homogeneity, and crystalline alignment (Debeaufort *et al.,* 1993).

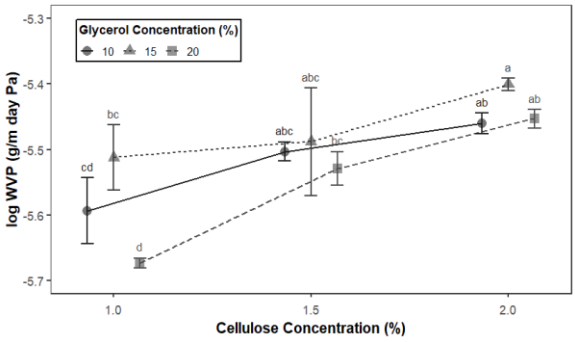


Fig. 5: Effect of Cellulose concentration and glycerol content on the WVP of starch-based bioplastic films

In this study, the WVP values of cellulose-based bioplastics ranged from 2.12 to 3.98 × 10^{-6} g/m·day·Pa (See Figure 5). The lowest permeability was recorded in the formulation containing 20% glycerol and 1.0% cellulose, which was significantly different from other groups ($p < 0.05$). Conversely, the formulation containing 15% glycerol and 2.0% cellulose exhibited the highest WVP, indicating weaker moisture-barrier properties. These findings align partially with previous work by Zhou *et al.*

(2025), who reported a lower WVP of 1.37 × 10^{-8} kg/m·day·Pa using alternative formulations.

The hydrophilic nature of cellulose likely contributes to elevated WVP by enhancing water molecule affinity (Mohammad Azmin *et al.,* 2020); however, when cellulose is incorporated in its nanoform, improved dispersion and hydrogen bonding within the matrix enhance the matrix's structure. This results in increased tortuosity of the diffusion pathway, ultimately reducing water vapor migration (Abe *et al.,* 2021). Guivier *et al.* (2024) also demonstrated a 76% reduction in WVP by incorporating multilayered nanocellulose into PLA films.

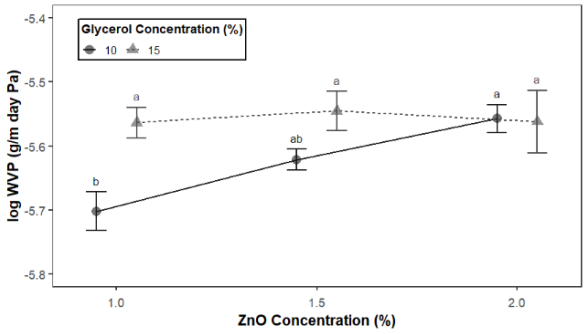


Fig. 6: Effect of ZnO concentration and glycerol content on the WVP of starch-based bioplastic films

Compared to cellulose, ZnO-based bioplastics exhibited a generally lower WVP, ranging from 1.98 to 2.85 × 10^{-6} g/m·day·Pa (See Figure 6). The formulation containing 10% glycerol and 1.0% ZnO yielded the best moisture barrier performance. Intermediate ZnO concentrations (1.5–2.0%) and higher glycerol levels (15%) tended to increase WVP. These values are consistent with findings by Vyas *et al.* (2025), who reported WVPs between 4.24 and 5.62 × 10^{-6} g/m·day·Pa for carboxymethyl cellulose-based films.

ZnO is known to act as a diffusion barrier by limiting molecular mobility, thereby reducing water vapor transport due to its relatively low hydrophilicity *(Anugrahwidya et al.,* 2022). Like cellulose, ZnO likely functions through a tortuosity-based mechanism, extending the path length for diffusing molecules (Ngo *et al.,* 2018). However, most WVP differences among ZnO formulations were not statistically significant ($p > 0.05$), suggesting that higher ZnO concentration may be required to achieve meaningful permeability reduction. Díez-Pascual (2024) identified 5% ZnO as an optimal threshold for minimizing WVP in bioplastics.

Glycerol content also significantly affected WVP values ($p < 0.05$). Increased glycerol concentration was associated with higher WVP, which is attributed to its plasticizing effect. Glycerol disrupts intermolecular interactions and enhances free volume within the matrix, thereby increasing water vapor mobility (Ballesteros-Mártinez *et al.,* 2020). In contrast, lower glycerol concentrations contribute to a more compact polymer network, reducing moisture diffusion (Tarique *et al.,* 2021). Interestingly, some studies report that higher glycerol levels can also facilitate hydrogen bonding with cellulose, potentially offsetting its plasticizing effect (Agustin *et al.,* 2024). This may explain why bioplastics with 20% glycerol exhibited slightly lower WVP than those with 10% or 15%, despite expectations to the contrary.

Best Formulation Determination

TOPSIS was employed to identify the optimal bioplastic formulation by integrating multiple performance indicators i.e. mechanical strength, transparency, and water vapor permeability (WVP). In this study, tensile strength and transparency were treated as beneficial criteria, while WVP was considered non-beneficial due to its inverse

relationship with barrier effectiveness.

Table 4. The TOPSIS score of cellulose-based bioplastic

Glycerol (%)	Cellulose (%)	Score
20	2	0.732
20	1.5	0.690
20	1	0.615
15	2	0.610
15	1.5	0.435
15	1	0.386
10	2	0.381
10	1.5	0.
10	1	0.324

As shown in Table 4, within the cellulose-based formulations, the highest-ranking formulation was obtained at 20% glycerol and 2% cellulose (TOPSIS score = 0.732). This formulation exhibited the highest tensile strength (1.87 MPa), accompanied by moderate transmittance (46.4%) and acceptable water vapor permeability (−5.45), indicating an overall optimal balance between mechanical strength and barrier properties.

The high ranking of this formulation suggests that increasing cellulose content up to 2% effectively enhanced the reinforcing effect within the polymer matrix, leading to improved tensile strength. Simultaneously, the presence of 20% glycerol likely contributed to sufficient plasticization, improving polymer chain mobility and preventing excessive brittleness. Although this formulation showed lower transmittance compared to others, the TOPSIS analysis indicates that mechanical performance and barrier properties had a stronger influence on the overall ranking.

Formulations with lower cellulose content (1–1.5%) at the same glycerol level demonstrated higher transmittance (51.4–57.5%) and lower WVP (−5.67), but were ranked lower due to reduced tensile strength. Conversely, formulations with lower glycerol content (10–15%) generally exhibited inferior mechanical properties, likely due to insufficient plasticization, which limited polymer chain flexibility and resulted in weaker film structures.

Table 5. The TOPSIS score of ZnO-based bioplastic

Glycerol (%)	ZnO (%)	Score
15	2	0.757
15	1.5	0.665
10	2	0.546
10	1.5	0.350
10	1	0.295
15	1	0.293

As shown in Table 5, for the ZnO-based formulations, the highest-ranking formulation was obtained at 15% glycerol and 2% ZnO (TOPSIS score = 0.757). This formulation demonstrated the highest tensile strength (1.68 MPa), along with moderate transmittance (51.6%) and competitive water vapor permeability (−5.56), indicating a well-balanced combination of mechanical and barrier properties.

The superior ranking of this formulation suggests that ZnO at 2% effectively reinforced the polymer matrix, enhancing tensile strength without excessively compromising other functional properties. At the same time, the presence of 15% glycerol appears sufficient to plasticize the system, improving flexibility while maintaining structural integrity. Although the transmittance was not the highest among the tested formulations, the TOPSIS results indicate that mechanical performance played a more dominant role in determining the optimal formulation.

The second-ranked formulation (1.5% ZnO, 15% glycerol) showed a comparable

balance across all parameters, but its slightly lower tensile strength (1.47 MPa) resulted in a reduced overall score. In contrast, formulations with lower glycerol content (10%) generally exhibited reduced tensile strength, likely due to insufficient plasticization, which limited polymer chain mobility. Meanwhile, increasing transparency observed in some lower-ranked formulations (e.g., 10% glycerol, 1% ZnO) was accompanied by weaker mechanical properties, reducing their overall suitability.

The integration of the t-test results (Table 6) provides statistical validation for the differences observed between cellulose- and ZnO-based bioplastics. For tensile strength, cellulose-based films exhibited significantly higher values (1.87 ± 0.03 MPa) compared to ZnO-based films (1.68 ± 0.05 MPa), with a mean difference of 0.19 MPa ($p = 0.0056$). This indicates that cellulose incorporation contributes more effectively to mechanical reinforcement, likely due to its fibrous structure, which enhances stress transfer within the polymer matrix.

In contrast, ZnO-based films showed significantly higher transparency (51.61 ± 1.18%) than cellulose-based films (46.40 ± 0.77%), with a mean difference of −5.21% ($p = 0.0052$). This result suggests that ZnO nanoparticles, when well-dispersed, interfere less with light transmission compared to cellulose particles, which tend to scatter light due to their larger particle size.

For water vapor permeability (log WVP), no statistically significant difference was observed between the two groups ($p = 0.0514$), although ZnO-based films showed a slightly lower (more negative) mean value. This indicates that both fillers provide comparable barrier performance within the tested formulation range.

Overall, these findings support the TOPSIS results by confirming that cellulose-based films are superior in mechanical strength, whereas ZnO-based films excel in optical properties. However, since barrier properties were statistically similar, the selection of the optimal formulation depends primarily on the desired balance between strength and transparency. Based on the TOPSIS analysis, the formulation containing 2% cellulose and 20% glycerol demonstrated the best overall performance, highlighting its potential suitability for applications requiring stronger yet moderately transparent biodegradable films.

Morphological Characteristic

The surface morphology of the bioplastics was examined using Scanning Electron Microscopy (SEM) at 500× magnification. As shown in Figure 7, notable differences were observed between cellulose- and ZnO-based films. The ZnO-based bioplastic exhibited a relatively smooth and uniform surface, indicative of effective nanoparticle dispersion within the starch matrix. In contrast, the cellulose-based bioplastic displayed a more fibrillar and heterogeneous texture, with visible aggregates likely due to the partial crystallinity and larger particle size of untreated cellulose fibers.

Table 6. Mean difference of cellulose and ZnO based bioplastic

Parameters	Mean (sd) of Cellulose	Mean (sd) of ZnO	Mean Difference	t (df)	p value	95% C.I.
Tensile strength (MPa)	1.87 (0.03)	1.68 (0.05)	0.09	5.84 (3.66)	0.0056	0.10, 0.29
Transparency (%)	46.40 (0.77)	51.61 (1.18)	-5.21	-6.49 (3.36)	0.0052	-7.62, -2.80
Log WVP (g/m day Pa)	-5.67 (0.01)	-5.70 (0.05)	-0.03	3.72 (2.33)	0.0514	-0.01, 0.22

This morphological difference may be attributed to the natural tendency of cellulose chains to form hydrogen bonds, leading to fiber aggregation and surface irregularities (Gea *et al.,* 2022). On the other hand, ZnO nanoparticles, due to their smaller size and better compatibility with the starch matrix, appear to distribute more evenly.

These surface characteristics can affect the mechanical behavior of the bioplastics. Rough or uneven surfaces in cellulose films may promote non-uniform stress distribution, potentially reducing tensile strength when aggregation becomes excessive. Previous research has shown that cellulose addition can increase tensile strength up to an optimal threshold (e.g., 5% loading), beyond which mechanical performance declines due to agglomeration (Abdel Hamid *et al.,* 2025). In contrast, although ZnO disperses more uniformly, it may interrupt the starch matrix continuity and does not contribute significantly to tensile reinforcement unless synergistically bonded. In PLA systems, for example, ZnO at 2 wt% provided a tensile strength of 22 MPa, comparable to or even lower than well-dispersed cellulose at similar concentrations (Akshaykranth *et al.,* 2025).

SEM observations support the conclusion that filler morphology and dispersion play crucial roles in the mechanical integrity of bioplastic films, with cellulose offering reinforcement potential at the cost of surface regularity, and ZnO contributing to smoother surfaces but with more limited structural reinforcement.

Chemical Characteristics

The FTIR spectra of both bioplastics exhibited several characteristic absorption bands indicating the presence of polysaccharide components and intermolecular interactions in the matrix (See Figure 8).

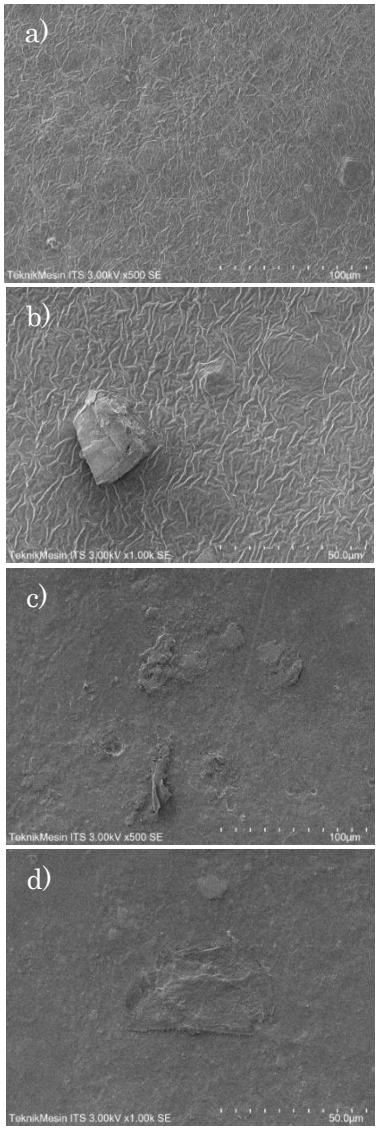


Fig. 7: SEM images of bioplastic films a) cellulose at 500×, b) cellulose at 1000×, c) ZnO at 500×, d) ZnO at 1000×

The molecular interactions between components in the bioplastics were analyzed using FTIR spectroscopy. Compared to native starch spectra, both cellulose- and ZnO-based films showed broad absorption around ~3280 cm^{-1}, corresponding to O–H stretching, with a noticeable shift, indicating enhanced hydrogen bonding between starch, glycerol, and the fillers. The cellulose-based sample exhibited a peak near ~2900 cm^{-1} (C–

H stretching) and strong bands around ~1020–1050 cm^{-1}, characteristic of C–O and C–C stretching in polysaccharides. The presence of ZnO was indicated by a weak absorption band near ~600 cm^{-1}, assigned to Zn–O vibrations, consistent with prior reports (Jannah *et al.,* 2019; Ranote *et al.*, 2024). These spectra confirm that filler incorporation did not introduce new chemical bonds but reinforced the existing matrix through physical interactions and hydrogen bonding.

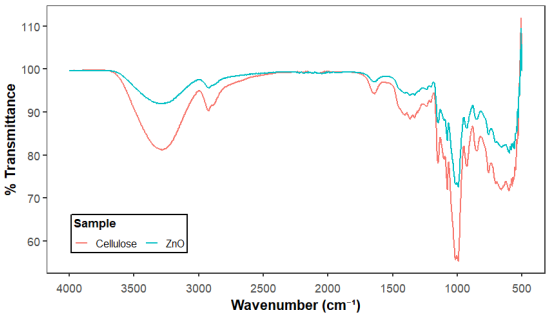


Fig. 8: Comparison of FTIR spectra of cellulose and ZnO bioplastics

To further understand the structural differences, XRD analysis was conducted (See Figure 9). The cellulose-based bioplastic showed a broad peak at 2θ ≈ 19°, indicating a semi-crystalline cellulose I structure. This pattern is typical of plant-derived cellulose and reflects a balance between crystalline and amorphous regions (Gea *et al.,* 2022; Karaca *et al.,* 2022). Compared with native starch-based films reported in previous studies (Werapun *et al.,* 2024), the addition of SCG-cellulose and ZnO resulted in a noticeable increase in peak intensity. This enhancement suggests an increase in the crystallinity index (CrI), as the fillers likely acted as nucleating agents, promoting a more ordered molecular arrangement within the starch matrix. The broadness of the peak suggests partial disruption of crystallinity due to blending with glycerol and starch, contributing to the film's flexibility.

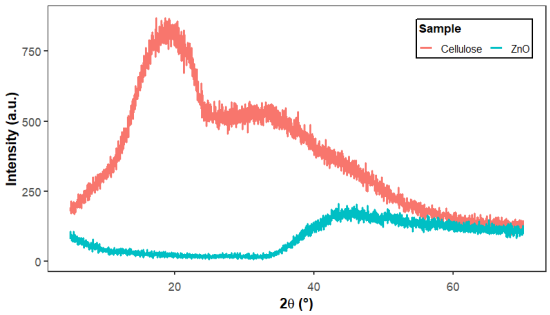


Fig. 9: Comparison of XRD spectra of cellulose and ZnO bioplastics

In contrast, the ZnO-based bioplastic presented sharp peaks at 2θ ≈ 31.7°, 34.4°, and 36.2°, which match the characteristic reflections of ZnO's wurtzite hexagonal crystal structure, as referenced in JCPDS card no. 36-1451. These peaks confirm the presence of crystalline ZnO and suggest that ZnO acts as a nucleating agent, enhancing the overall crystallinity of the bioplastic matrix (Anugrahwidya *et al.,* 2022; Asri *et al.,* 2020). Despite their high crystallinity, the ZnO peaks showed moderate intensity, possibly due to low filler concentration or uniform particle dispersion.

Together, the FTIR and XRD results confirm that both cellulose and ZnO were successfully integrated into the bioplastic matrix. While cellulose contributed to hydrogen bonding and moderate flexibility, ZnO enhanced crystallinity, potentially improving mechanical strength and barrier properties.

CONCLUSIONS

This study demonstrated the successful utilization of cellulose derived from spent coffee grounds (SCG) and zinc oxide (ZnO) as functional fillers in starch-based bioplastics. Both fillers significantly influenced the

mechanical, optical, and barrier properties of the bioplastics. Cellulose enhanced tensile strength due to its reinforcing semi-crystalline structure, while ZnO improved transparency and contributed to smoother film morphology. FTIR and XRD analyses confirmed the chemical interactions and crystallinity patterns associated with each filler, and SEM imaging revealed morphological differences that affected performance. The application of TOPSIS as a multi-criteria decision-making tool identified the formulation containing 1% SCG cellulose and 20% glycerol as the optimal composition. These results highlight the feasibility of converting agro-industrial waste into value-added, biodegradable materials with potential for sustainable packaging applications. Further research may focus on long-term biodegradability or migration tests to assess safety in food contact applications.

ACKNOWLEDGEMENT

The support provided by the chemistry and processing laboratory, as well as fellow staff of the Food Technology Program, Ciputra University Surabaya, is hereby gratefully acknowledged. School of Tourism funded this research with grant number 036/UC-SoT/ST/IV/2025.

REFERENCES

Abdel Hamid, E.M., Mohamed, A.E., Mohamed, A.A., Galal, A.A., Mekhemr, A.A., Saleh, E.S., Hassan, M.I., Ahmed, M.H., Elgendy, S.K., 2025. "Optimization of corn starch/glycerol, acetic acid, and cellulose fibers ratio on biodegradable plastic synthesis by Box–Behnken design (BBD)." *Clean Technol. Environ. Policy, 27,* 4433-4455. https://doi.org/10.1007/s10098-025-03135-7

Abdullah, A.H., Putri, O.D., Fikriyyah, A., Nissa, R., Hidayat, S., Septiyanto, R., Karina, M., Satoto, R., 2020. "Harnessing the excellent mechanical, barrier and antimicrobial properties of zinc oxide (ZnO) to improve the performance of starch-based bioplastic." *Polym. Technol. Mater., 59,* 1259–1267. https://doi.org/10.1080/25740881.2020.1738466

Abe, M.M., Martins, J.R., Sanvezzo, P.B., Macedo, J. V, Branciforti, M.C., Halley, P., Botaro, V.R., Brienzo, M., 2021. "Advantages and disadvantages of bioplastics production from starch and lignocellulosic components." Polymers, 13(15), 2484. https://doi.org/10.3390/polym13152484

Agustin, S., Cahyanto, M.N., Wahyuni, E.T., Supriyadi, 2024. "Effect of glycerol plasticizer on the structure and characteristics of bacterial cellulose-based biocomposite films." *IOP Conf. Ser. Earth Environ. Sci.,* 1377. https://doi.org/10.1088/1755-1315/1377/1/012046

Akshaykranth, A., Ajayan, J., Anitha, N., 2025. "Development of biodegradable PLA/Nanoclay/ZnO polymer films for future Industrial packaging applications." *Results Surf. Interfaces, 19,* 100518. https://doi.org/https://doi.org/10.1016/j.rsurfi.2025.100518

Ali, S., Mehra, V., Eltaggaz, A., Deiab, I., Pervaiz, S., 2024. "Optimization and prediction of additively manufactured PLA-PHA biodegradable polymer blend using TOPSIS and GA-ANN." *Manuf. Lett., 41,* 795–802. https://doi.org/https://doi.org/10.1016/j

.mfglet.2024.09.099

Ali, S.S., Elsamahy, T., Abdelkarim, E.A., Abdelfattah, A., Ramadan, H., Mostafa, S., Metwally, S.M., Sun, J., 2023. 12 - Engineered yeast for the production of bioplastics, in: Daverey, A., Dutta, K., Joshi, S., Gea, T.B.T.-A. in Y.B. for B. and S. (Eds.), Elsevier, pp. 277–296. https://doi.org/https://doi.org/10.1016/B978-0-323-95449-5.00017-5

Anugrahwidya, R., Armynah, B., Tahir, D., 2022. "Composites bioplastic film for various concentration of zinc oxide (ZnO) nanocrystals towards physical properties for high biodegradability in soil and seawater." *J. Polym. Environ., 30,* 2589–2601. https://doi.org/10.1007/s10924-021-02363-4

Arifin, H.R., Djali, M., Nurhadi, B., Azlin-Hasim, S., Masruchin, N., Vania, P.A., Hilmi, A., 2022. "Corn starch-based bionanocomposite film reinforced with ZnO nanoparticles and different types of plasticizers." *Front. Sustain. Food Syst., 6,* 886219. https://doi.org/10.3389/fsufs.2022.886219

Armynah, B., Anugrahwidya, R., Tahir, D., 2022. "Composite cassava starch/chitosan/Pineapple Leaf Fiber (PALF)/Zinc Oxide (ZnO): Bioplastics with high mechanical properties and faster degradation in soil and seawater." *Int. J. Biol. Macromol., 213,* 814–823. https://doi.org/https://doi.org/10.1016/j.ijbiomac.2022.06.038

Asri, N., Yuniati, Y., Hindarso, H., Suprapto, S., Yogaswara, R., 2020. "Biodiesel production from Kesambi (*Schleichera oleosa*) oil using multi-walled carbon nanotubes supported zinc oxide as a solid acid catalyst." *IOP Conf. Ser. Earth Environ. Sci.*, *456,* 12003. https://doi.org/10.1088/1755-1315/456/1/012003

Atiwesh, G., Mikhael, A., Parrish, C.C., Banoub, J., Le, T.-A.T., 2021. "Environmental impact of bioplastic use: A review." *Heliyon, 7(9),* e07918. https://doi.org/https://doi.org/10.1016/j.heliyon.2021.e07918

Azlim, N.A., Mohammadi Nafchi, A., Oladzadabbasabadi, N., Ariffin, F., Ghalambor, P., Jafarzadeh, S., Al-Hassan, A.A., 2022. "Fabrication and characterization of a pH-sensitive intelligent film incorporating dragon fruit skin extract." *Food Sci. Nutr., 10*, 597–608. https://doi.org/10.1002/fsn3.2680

Ballesteros-Mártinez, L., Pérez-Cervera, C., Andrade-Pizarro, R., 2020. "Effect of glycerol and sorbitol concentrations on mechanical, optical, and barrier properties of sweet potato starch film." *Nutr. Food Sci. J., 20,* 1–9. https://doi.org/https://doi.org/10.1016/j.nfs.2020.06.002

Baltscheit, J., Schmidt, N., Schröder, F., Meyer, J., 2020. "Investigations on the aging behavior of transparent bioplastics for optical applications." *InfoMat, 2,* 424–433. https://doi.org/https://doi.org/10.1002/inf2.12065

Benitez, J.J., Florido-Moreno, P., Porras-Vázquez, J.M., Tedeschi, G., Athanassiou, A., Heredia-Guerrero, J.A., Guzman-Puyol, S., 2024. "Transparent, plasticized cellulose-glycerol bioplastics for food packaging applications." *Int. J. Biol. Macromol., 273,* 132956. https://doi.org/https://doi.org/10.1016/j.ijbiomac.2024.132956

Cabernard, L., Pfister, S., Oberschelp, C., Hellweg, S., 2022. Growing

environmental footprint of plastics driven by coal combustion. *Nat. Sustain., 5,* 139–148. https://doi.org/10.1038/s41893-021-00807-2

Dadashi, P., Torbatinejad, K., Babaei, A., 2025. "Hybridization as a promising approach to engineering the desired performance of bio-nanocomposites: GO-ZnO hybrid reinforced PCL." *Sci. Rep., 15,* 17259. https://doi.org/10.1038/s41598-025-02087-8

Debeaufort, F., Martin-Polo, M., Voilley, A., 1993. "Polarity homogeneity and structure affect water vapor permeability of model edible films." *J. Food Sci., 58,* 426–429. https://doi.org/https://doi.org/10.1111/j.1365-2621.1993.tb04290.x

Devika, R., Saha, R., 2024. "Characterization and optimization studies of cellulose-based bioplastics extracted from *Musa paradisiaca L*." *Glob. Nest J., 26 (2),* 1-10. https://doi.org/10.30955/gnj.005613

Dibha, A., MASRURI, M., Srihardyastutie, A., 2023. "Degradable bioplastic developed from pine-wood nanocellulose as a filler combined with orange peel extract." *Indones. J. Chem., 23(1),* 127–139. https://doi.org/10.22146/ijc.75520

Folino, A., Pangallo, D., Calabrò, P.S., 2023. "Assessing bioplastics biodegradability by standard and research methods: Current trends and open issues." J. *Environ. Chem. Eng., 11,* 109424. https://doi.org/https://doi.org/10.1016/j.jece.2023.109424

Fransiska, D., Abdullah, A.H.D., Nurhayati, Irianto, H.E., Nissa, R.C., Sedayu, B.B., Syamani, F.A., Raharjo, S., Suwarti, Agusman, 2024. "Impact of agar–glycerol ratios on the physicochemical properties of biodegradable seaweed films: A compositional study." *Int. J. Biol. Macromol., 280,* 135855. https://doi.org/https://doi.org/10.1016/j.ijbiomac.2024.135855

Gea, S., Meldawati Pasaribu, K., Sarumaha, A., Rahayu, S.R.I., 2022. "Cassava starch/bacterial cellulose-based bioplastics with Zanthoxylum acanthopodium." *Biodiversitas J. Biol. Divers., 23 (5)*, 2601-2608. https://doi.org/10.13057/biodiv/d230542

Gonçalves, S.M., dos Santos, D.C., Motta, J.F.G., Santos, R.R. dos, Chávez, D.W.H., Melo, N.R. de, 2019. Structure and functional properties of cellulose acetate films incorporated with glycerol. *Carbohydr. Polym., 209*, 190–197. https://doi.org/https://doi.org/10.1016/j.carbpol.2019.01.031

Guivier, M., Chevigny, C., Domenek, S., Casalinho, J., Perré, P., Almeida, G., 2024. "Water vapor transport properties of bio-based multilayer materials determined by original and complementary methods." *Sci. Rep., 14, 50.* https://doi.org/10.1038/s41598-023-50298-8

Guzman-Puyol, S., Benítez, J.J., Heredia-Guerrero, J.A., 2022. "Transparency of polymeric food packaging materials." *Food Res. Int., 161,* 111792. https://doi.org/https://doi.org/10.1016/j.foodres.2022.111792

Hamidy, R., Rachman, H., Anggara, J., Sulistyo, J., Asri, N., 2025. "Extraction and Characterization of cellulose from arabica spent coffee grounds." *J. IPTEK, 29,* 95–104. https://doi.org/10.31284/j.iptek.2025.v29i1.7815

Hasna, T., Lestari, C., Putri, W., Fathuroya, V., 2022. "The effect of ZnO (zinc oxide) and

glycerol concentrations on the mechanical properties of bioplastics made from Canna tuber (*Canna edulis*) starch." *Adv. Food Sci. Sustain. Agric. Agroindustrial Eng., 5,* 21–28. https://doi.org/10.21776/ub.afssaae.2022.005.01.2

Hernandez, C., Rosa, D., 2016. Extraction of cellulose nanowhiskers: natural fibers source, methodology and application. Polymer Science: Research Advances, Practical Applications And Educational Aspects. Formatex Research Center, Brazil. pp. 232–242.

Janas, S., Kowalska, M., 2023. "Accuracy of drying selected products using a moisture analyzer method based on infrared radiation." *Metrol. Meas. Syst., 30 (2),* 305–321. https://doi.org/10.24425/mms.2023.144873

Jannah, M., Ahmad, A., Hayatun, A., Taba, P., Chadijah, S., 2019. "Effect of filler and plastisizer on the mechanical properties of bioplastic cellulose from rice husk." *J. Phys. Conf. Ser., 1341*, 32019. https://doi.org/10.1088/1742-6596/1341/3/032019

Karaca, A.E., Özel, C., Özarslan, A.C., Yücel, S., 2022. "The simultaneous extraction of cellulose fiber and crystal biogenic silica from the same rice husk and evaluation in cellulose-based composite bioplastic films." *Polym. Compos., 43*, 6838–6853. https://doi.org/https://doi.org/10.1002/pc.26729

Karmee, S.K., 2018. "A spent coffee grounds based biorefinery for the production of biofuels, biopolymers, antioxidants and biocomposites." *Waste Manag., 72,* 240–254. https://doi.org/https://doi.org/10.1016/j.wasman.2017.10.042

Khouaja, A., Koubaa, A., Ben Daly, H., 2025. "Mechanical and morphological properties of cellulose biocomposites." *Chemosphere, 379,* 144415. https://doi.org/https://doi.org/10.1016/j.chemosphere.2025.144415

Klink, M.J., Laloo, N., Leudjo Taka, A., Pakade, V.E., Monapathi, M.E., Modise, J.S., 2022. "Synthesis, characterization and antimicrobial activity of zinc oxide nanoparticles against selected waterborne bacterial and yeast pathogens." *Molecules, 27(11),* 3532. https://doi.org/10.3390/molecules27113532

Krishnamurthy, A., Amritkumar, P., 2019. "Synthesis and characterization of eco-friendly bioplastic from low-cost plant resources." *SN Appl. Sci., 1,* 1432. https://doi.org/10.1007/s42452-019-1460-x

Lee, S.W., Said, N.S., Sarbon, N.M., 2021. "The effects of zinc oxide nanoparticles on the physical, mechanical and antimicrobial properties of chicken skin gelatin/tapioca starch composite films in food packaging." *J. Food Sci. Technol., 58,* 4294–4302. https://doi.org/10.1007/s13197-020-04904-6

Liu, Y.-R., Tang, X., Zeng, Q., Lai, J.-P., 2024. "Impacts of ultraviolet absorption by zinc oxide nanoparticle modifiers on asphalt aging." *Sci. Rep., 14,* 19918. https://doi.org/10.1038/s41598-024-70875-9

Long, J., Zhang, W., Zhao, M., Ruan, C.-Q., 2023. "The reduce of water vapor permeability of polysaccharide-based films in food packaging: A comprehensive review." *Carbohydr. Polym., 321,* 121267. https://doi.org/https://doi.org/10.1016/j

.carbpol.2023.121267

Lounis, F.M., Benhacine, F., Hadj-Hamou, A.S., 2024. "Improving water barrier properties of starch based bioplastics by lignocellulosic biomass addition: Synthesis, characterization and antibacterial properties." *Int. J. Biol. Macromol., 283,* 137823. https://doi.org/https://doi.org/10.1016/j.ijbiomac.2024.137823

Mohammad Azmin, S.N.H., Aliah, N., Mat Nor, M.S., 2020. Development and "Characterization of food packaging bioplastic film from cocoa pod husk cellulose incorporated with sugarcane bagasse fibre." *J. Bioresour. Bioprod., 5*, 259–266. https://doi.org/10.1016/j.jobab.2020.10.003

Nasution, H., Elisa, J., Dalimunthe, N., Asdita, M., Zoelva, A., Sartika, M., 2023. "The role of stirring speed on the properties improvement of bioplastic composite sagu starch modified with cellulose microcrystal and betel leaf extract." *RASAYAN J. Chem., 16,* 1912–1919. https://doi.org/10.31788/RJC.2023.1638261

Nayanathara Thathsarani Pilapitiya, P.G.C., Ratnayake, A.S., 2024. "The world of plastic waste: A review." *Clean. Mater., 11*, 100220. https://doi.org/https://doi.org/10.1016/j.clema.2024.100220

Ngo, T.M.P., Dang, T.M.Q., Tran, T.X., Rachtanapun, P., 2018. "Effects of zinc oxide nanoparticles on the properties of pectin/alginate edible films." *Int. J. Polym. Sci., 2018*, 5645797. https://doi.org/https://doi.org/10.1155/2018/5645797

Nigam, S., Das, A.K., Patidar, M.K., 2021. "Synthesis, characterization and biodegradation of bioplastic films produced from Parthenium hysterophorus by incorporating a plasticizer (PEG600)." *Environ. Challenges, 5,* 100280. https://doi.org/https://doi.org/10.1016/j.envc.2021.100280

Nurhayati, I., Kurniawati, C.T., Kholif, M. Al, 2025. "Sustainable bioplastics from sweet corn cob waste: Influence of zinc oxide and glycerol on mechanical properties and biodegradability." Indones. *J. Environ. Manag. Sustain., 9,* 1–11. https://doi.org/10.26554/ijems.2025.9.1.1-11

Oluwasina, Olugbenga, Aderibigbe, A., Ikupoluyi, S., Oluwasina, Olayinka, Ewetumo, T., 2024. "Physico-electrical properties of starch-based bioplastic enhanced with acid-treated cellulose and graphene oxide fillers." *Sustain. Chem. Environ., 6,* 100093. https://doi.org/https://doi.org/10.1016/j.scenv.2024.100093

Popescu, M.-C., Dogaru, B.-I., Popescu, C.-M., 2020. "Effect of cellulose nanocrystals nanofiller on the structure and sorption properties of carboxymethyl cellulose–glycerol–cellulose nanocrystals nanocomposite systems." *Materials, 13(13),* 2900. https://doi.org/10.3390/ma13132900

Putranti, L., Nugraheni, P., 2023. "Effect of carboxymethyl cellulose addition on the characteristic of chitosan-based bioplastic." *IOP Conf. Ser. Earth Environ. Sci., 1289,* 12038. https://doi.org/10.1088/1755-1315/1289/1/012038

Rahmatullah, R., Putri, R., Rendana, M., Waluyo, U., Andrianto, T., 2022. Effect of plasticizer and concentration on

characteristics of bioplastic based on cellulose acetate from kapok (*Ceiba pentandra*)." *Fiber. Sci. Technol. Indones., 7,* 73–83. https://doi.org/10.26554/sti.2022.7.1.73-83

Ranote, S., Kowalczuk, M., Guzenko, N., Duale, K., Chaber, P., Musioł, M., Jankowski, A., Marcinkowski, A., Kurcok, P., Chauhan, G.S., Chauhan, S., Kumar, K., 2024. "Towards scalable and degradable bioplastic films from Moringa oleifera gum/poly(vinyl alcohol) as packaging material." *Int. J. Biol. Macromol., 269,* 132219. https://doi.org/https://doi.org/10.1016/j.ijbiomac.2024.132219

Safitri, A., Sinaga, P.S.D., Nasution, H., Harahap, H., Masyithah, Z., Iriany, Hasibuan, R., 2022. "The role of various plastisizers and fillers additions in improving tensile strength of starch-based bioplastics: A mini review." *IOP Conf. Ser. Earth Environ. Sci., 1115*, 12076. https://doi.org/10.1088/1755-1315/1115/1/012076

Sanyang, M.L., Sapuan, S.M., Jawaid, M., Ishak, M.R., Sahari, J., 2016. "Effect of plasticizer type and concentration on physical properties of biodegradable films based on sugar palm (*Arenga pinnata*) starch for food packaging." *J. Food Sci. Technol., 53,* 326–336. https://doi.org/10.1007/s13197-015-2009-7

Sapei, L., Padmawijaya, K., Sijayanti, O., "Wardhana, P., 2017. Study of the influence of ZnO addition on the properties of chitosan-banana starch bioplastics." *IOP Conf. Ser. Mater. Sci. Eng., 223,* 12044. https://doi.org/10.1088/1757-899X/223/1/012044

Singh, T., Pal, N., Sharma, P., Passari, A., 2023. "Spent coffee ground: transformation from environmental burden into valuable bioactive metabolites. Rev. Environ." *Sci. Bio/Technology, 22,* 887–898. https://doi.org/10.1007/s11157-023-09669-w

Steven, S., Fauza, A.N., Mardiyati, Y., Santosa, S.P., Shoimah, S.M., 2022. Facile preparation of cellulose bioplastic from *Cladophora sp*. algae via hydrogel method. *Polymers, 14(21),* 4699 . https://doi.org/10.3390/polym14214699

Tagudin, N.M.F.B.A., Ibrahim, N.B., 2025. "Synthesis of polylactic acid from apple, pineapple, and potato residues." *ASEAN J. Chem. Eng., 25(1),* 75-86.. https://doi.org/10.22146/ajche.16580

Tamimi, N., Mohammadi Nafchi, A., Hashemi-Moghaddam, H., Baghaie, H., 2021. "The effects of nano-zinc oxide morphology on functional and antibacterial properties of tapioca starch bionanocomposite." *Food Sci. Nutr., 9,* 4497–4508. https://doi.org/10.1002/fsn3.2426

Tarique, J., Sapuan, S.M., Khalina, A., 2021. "Effect of glycerol plasticizer loading on the physical, mechanical, thermal, and barrier properties of arrowroot (*Maranta arundinacea*) starch biopolymers." *Sci. Rep., 11,* 13900. https://doi.org/10.1038/s41598-021-93094-y

Viana Freitas, V., Borges, L., Vidigal, M., Santos, M., Stringheta, P., 2024. "Coffee: A comprehensive overview of origin, market, and the quality process." Trends *Food Sci. Technol., 146*, 104411. https://doi.org/10.1016/j.tifs.2024.104411

Vyas, A., Ng, S., Fu, T., Anum, I., 2025. ZnO-Embedded carboxymethyl cellulose

bioplastic film synthesized from sugarcane bagasse for packaging applications." *Polymers*, *17(5),* 579. https://doi.org/10.3390/polym17050579

Werapun, U., Werapun, W., Phatthiya, A., 2024. "Characterization of composite bioplastic from Cassava starch with titanium dioxide and zinc oxide." *Dig. J. Nanomater. Biostructures, 19,* 275–282. https://doi.org/10.15251/DJNB.2024.191.275

Xie, D., Zhang, R., Zhang, C., Yang, S., Xu, Z., Song, Y., 2023. "A novel, robust mechanical strength, and naturally degradable double crosslinking starch-based bioplastics for practical applications." *Int. J. Biol. Macromol., 253*, 126959. https://doi.org/https://doi.org/10.1016/j.ijbiomac.2023.126959

Yahia, R., Owda, M.E., Abou-Zeid, R.E., Abdelhai, F., El-Gamil, H.Y., Abdo, A.M., Ali, A.A., 2024. "Biodegradable, UV absorber and thermal stable bioplastic films from waxy corn starch/polyvinyl alcohol blends." *Biomass Convers. Biorefinery, 14,* 27989–28006. https://doi.org/10.1007/s13399-022-03683-8

Zhou, S.-J., Xiong, S.-J., Wang, H.-M., Yu, S., Yuan, T.-Q., 2025. "Direct utilization of cassava flour in biodegradable films: The compatibilizing effect of cassava protein on poly (butylene adipate-co-terephthalate) and cassava starch." *Int. J. Biol. Macromol., 319,* 145532. https://doi.org/https://doi.org/10.1016/j.ijbiomac.2025.145532